Heart Rate Estimation From Wrist-Worn Photoplethysmography: A Review

Dwaipayan Biswas, Neide Simões-Capela, Chris Van Hoof, and Nick Van Helleputte, *Member, IEEE*

***Abstract*— Photoplethysmography (PPG) is a low-cost, non-invasive, and optical technique used to detect blood volume changes in the microvascular tissue bed, measured from the skin surface. It has traditionally been used in commercial medical devices for oxygen saturation, blood pressure monitoring, and cardiac activity for assessing peripheral vascular disease and autonomic function. There has been a growing interest to incorporate PPG sensors in daily life, capable of use in ambulatory settings. However, inferring cardiac information (e.g. heart rate) from PPG traces in such situations is extremely challenging, because of interferences caused by motion. Following the IEEE Signal Processing Cup in 2015, numerous methods have been proposed for estimating particularly the average heart rate using wrist-worn PPG during physical activity. Details on PPG technology, sensor development, and applications have been well documented in the literature. Hence, in this paper, we have presented a comprehensive review of state-of-the-art research on heart rate estimation from wrist-worn PPG signals. Our review also encompasses brief theoretical details about PPG sensing and other potential applications–biometric identification, disease diagnosis using wrist PPG. This paper will set a platform for future research on pervasive monitoring using wrist PPG.**

***Index Terms*— Photoplethysmography (PPG), heart rate (HR), heart rate variability (HRV), atrial fibrillation (AF), pervasive, Internet of things (IoT).**

I. Introduction

ADVANCEMENTS in wireless sensor network (WSN) technologies have enabled continuous physiological sensing, aimed towards remote health monitoring [1], [2]. Cardiovascular disease (CVD) monitoring, one of the key research areas using wearable sensors, has primarily focused on electrocardiography (ECG) for heart rate (HR) monitoring, disease prognosis (e.g. arrhythmia, tachycardia, etc.) as well as biometric identification [3]–[5]. Research has also adopted photoplethysmography (PPG) sensors, gaining prominence owing to the commercial development of wrist-worn sensing modalities - smart watches and fitness trackers [6]–[10]. PPG based HR monitors present a popular alternative to ECG, as the former can be placed across various body locations such as earlobes, fingertips or wrist, making them convenient for ambulant daily usage [11].

PPG works on the principle of pulse oximetry, wherein a sensor emits light to the skin and measures the intensity of light which is reflected back or transmitted through the skin. PPG signal variations are caused by changes in arterial blood volume. The amplitude of the variations depend on the amount of blood rushing into the peripheral vascular bed, the optical absorption of blood, skin pigmentation, ambient light and the wavelength used to illuminate the blood (e.g. infrared, green, etc.) [11]– [13]. The cardiac rhythm corresponds to the periodicity of the PPG signal, which can be used towards estimating HR. Knowledge of HR aids in fitness tracking and can act as periodic intervention mechanism in CVD monitoring.

PPG signals acquired from wrist, in ambulant environment, are susceptible to motion artifacts (MA). MA is generally caused by movement of the sensor module relative to the skin, along with sensor deformation resulting from long-term daily usage. Thus, affecting signal quality and corresponding extraction of physiological parameters. A number of research initiatives in recent years have been successful in detecting, removing or attenuating MA, and estimating HR using time/frequency domain signal processing techniques as well as machine learning based approaches [14]–[16]. This has mainly been aided by the IEEE Signal Processing Cup (SPC) database from 2015 [17], with 23 PPG records acquired during both running and intense physical activity. Further developments have been reported on instantaneous HR, necessary for Heart Rate Variability (HRV) assessment [18]. Embedded PPG algorithms, targeting energy efficiency on resource-constrained sensing platform, have also received due attention [19].

There is extensive coverage on ECG signal processing encompassing various aspects of CVD research [20]–[23]. PPG sensing modalities have also been well covered in literature, detailing instrumentation and signal analysis [11], [24]–[26]. However, there has been a significant change in processing requirements with the advent of wrist-PPG affected by MA, giving rise to a host of spectral estimation techniques for computing HR with high fidelity [14], [16], [27]–[29]. Hence, in this article we focus on algorithmic developments using wrist PPG only, primarily centered around SPC database. The paper is organized as follows: details on PPG acquisition have been outlined in section II;

Manuscript received March 20, 2019; revised April 23, 2019; accepted April 28, 2019. Date of publication May 1, 2019; date of current version July 17, 2019. The associate editor coordinating the review of this paper and approving it for publication was Prof. Danilo Demarchi. *(Corresponding author: Dwaipayan Biswas.)*

The authors are with the Biomedical Circuits and Systems Group, IMEC, 3001 Heverlee, Belgium (e-mail: dwaipayan.biswas@imec.be; neide.simoescapela@imec.be; chris.vanhoof@imec.be; nick.vanhelleputte@imec.be).

Digital Object Identifier 10.1109/JSEN.2019.2914166

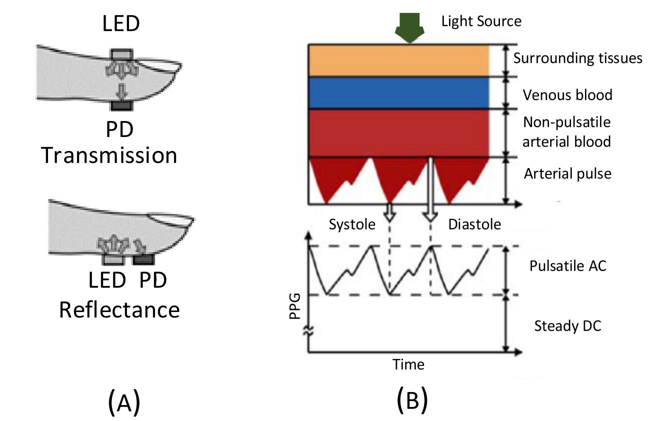

Fig. 1. (A) Light-emitting diode (LED) and photodetector (PD) placement for transmission and reflectance-mode photoplethysmography (PPG) [24]. (B) Variation in light attenuation by tissue [34].

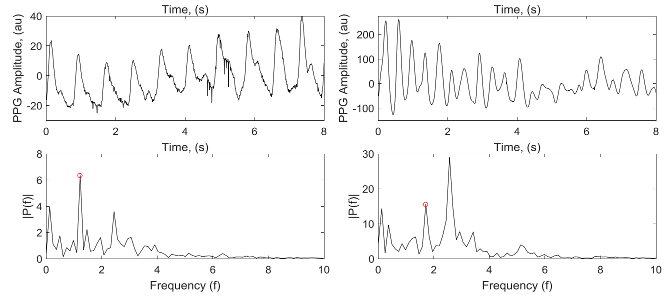

Fig. 2. Raw PPG signal and spectrum while walking (left) and during transition from walking to running (right), respectively. The highest PPG spectral peak does not coincide with true HR (highlighted) during intense motion.

HR estimation algorithms are presented in Section III; developments on wrist PPG applications-biometric identification and disease management are outlined in Section IV, with conclusions drawn in Section V.

II. PPG Signal Acquisition

The term photoplethysmography was first coined by Hertzman [30], representing blood volume changes in the dermal vasculature, owing to the pulsatile nature of the circulatory system [13], [31]. PPG requires a light source, a light emitting diode (LED), to illuminate the tissue and a photodetector (photodiode) to sense the minute variations in reflected or transmitted (cf. Fig. 1(A)) light intensity associated with perfusion changes in the catchment volume [24]. Different optical wavelengths interact differently with blood and tissues, involving several physical processes, i.e. scattering, absorption, reflection, transmission and fluorescence [32]. Hence correct selection of the light source wavelength is of prime importance [26]. Red, near-infra red (IR) and green light sources are typically employed in PPG sensors. Green light, having shorter wavelength, is less influenced by deep tissue movements and produces large intensity variations to cardiac modulations [33]. It exhibits greater absorption for oxyhemoglobin/deoxyhemoglobin, yielding a better signal-to-noise ratio (SNR), ensuring higher accuracy of pulse detection compared to red or IR, especially for micro-motions.

A transmitive sensor system (cf. Fig. 1(A), top) comprises LED and PD configured opposite to each other on the measurement surface (e.g. finger). On the other hand, a reflective system (cf. Fig. 1(A), bottom) has LED and PD configured sideways, making them popular with pervasive measurement sites, since they can be placed on any skin surface of the human body. However, movements further corrupt reflection-mode PPG, limiting physiological interpretation. The detected signal can be split into two components as shown in Fig. 1(B): (i) DC component, originating from constant absorbance by skin pigmentation, fat, muscle, bone and (ii) AC component caused due to cardiac-induced variations in blood volume related to the cardiac cycle (systole and diastole). The AC amplitude is influenced by the pressure exerted on skin (contact force between sensor and measurement site), which deforms the arterial geometry. Hence, the sensor must be attached firmly to a flat skin surface for accurate measurement.

A. PPG Databases

In Table I, we highlight publicly available databases with wrist-PPG signals which aided research activities.

III. HR Estimation From PPG

Motion is often an arbitrary and spontaneous behavior which can be aperiodic (e.g. cooking) or periodic (e.g. running). When acquired in ambulant environment, PPG signals exhibit both MA spectral peaks that lie distant from HR spectral peak, as well as overlapping ones, rendering them indistinguishable. The effect of MA is further depicted in Fig. 2. Hence, MA removal methodologies assume significance for extracting vital cardiac information. In this section we present an overview of: (a) commonly used MA removal techniques and evaluation metrics, (b) key HR estimation algorithms reportedly evaluated on SPC database, (c) algorithms targeting reduced computational complexity, (d) machine learning based algorithms, (e) brief review on commercial devices using wrist-PPG, and, lastly (f) HRV estimation.

A. MA Removal Techniques and Evaluation Metrics

HR estimation from artifact-induced PPG signals has been researched extensively [16], [36] using a range of methods including adaptive filtering [36]–[39], independent component analysis (ICA) [40], frequency-domain ICA [41], empirical mode decomposition (EMD) [28], [42], wavelet-based denoising [43], or other decomposition models [27], [44], spectral subtraction [45], [46], and Kalman filtering [47]. ICA, although a popular blind source separation methodology holds the assumption of statistical independence between the PPG signal and MA, which does not always hold true and hence is not an effective technique [48]. Using adaptive filtering (recursive least squares-RLS, normalized least mean squares-NLMS and variable step-size least mean squares) to weaken MA with the aid of other signals (e.g. acceleration) that correlate closely with motion but not the PPG signal has also been popular [39], [49]. However, the performance of some

TABLE I
WRIST-PPG PUBLIC DATABASES

Ref	Database	Protocol
[17]	IEEE Signal Processing Competition (SPC)– Training	• 12 male subjects, yellow skin, 18-35 years • wristband embedding: ▪ 2-channel PPG (pulse oximeter with 609 nm green LED) ▪ 3-axis acceleration • ECG recorded simultaneously from the chest (used as reference for HR) • all signals sampled at 125 Hz • subjects walked or ran on a treadmill in order: ▪ 1–2 km/h for 0.5 min, ▪ 6–8 km/h for 1 min, ▪ 12–15 km/h for 1 min, ▪ 6–8 km/h for 1 min, ▪ 12–15 km/h for 1 min, ▪ 1–2 km/h for 0.5 min. • subjects used the hand to pull clothes, wipe sweat on forehead, and push buttons on the treadmill, in addition to freely swing.
[17]	IEEE Signal Processing Competition (SPC) – Testing	• 11 subjects, aged 19-58 years • wrist PPG acquired using a pulse oximeter with green LEDs • 3-axis accelerometer • ECG simultaneously recorded from chest • all signals sampled at 125 Hz • five minutes recording of intensive arm movements • subjects performed various commonly used arm rehabilitation exercises, running, jump, push-up and boxing.
[35]	Wrist PPG during exercise (University of Manchester)	• 9 subjects in total (with only 1 subject participating in all exercises) • wrist PPG signal (510 nm green LED) • Two 3-axis accelerometers with ±2 g low-noise and ±16 g wide-range for capturing various exercise situations • 3-axis gyroscope for orientation • ECG signal captured from chest • 4 different exercise conditions: ▪ walking on a treadmill, ▪ running on a treadmill, ▪ exercise bike set to a low resistance (high cycling speeds), ▪ exercise bike set to a high resistance (low cycling speeds).
[92]	Wrist PPG during walking/running (Wonkwang University)	• 24 subjects (10 males, 14 females), average age of 26.9 ± 4.8 years • 3-channel wrist PPG (525 nm green LED) • 3-axis accelerometers • 3-axis gyroscope • ECG signal captured using Holter device • all signals sampled at 50 Hz • Modified Bruce protocol: ▪ 2 mins walking on a treadmill, ▪ 3 mins of running, ▪ 2 mins of walking, ▪ 3 mins of running, ▪ 2 mins of walking to cool down.

of these adaptive techniques were verified for relatively small movements, with the sensor placed at fingertip or forehead, as compared to the wrist, where the performance was low during physical exercise [36], [39].

Performance evaluation of the algorithms were carried out with respect to ground truth HR, obtained from simultaneously recorded ECG signal. Given a time window, the number of cardiac cycles H (manually selecting the R-peaks) and the associated duration D (in seconds) are used to calculate the true HR (HR_{true}) as 60H/D (in beat per minute, BPM). The Absolute Error (AE) is used to evaluate the accuracy of each HR estimate, where HR_{est} and HR_{true} are the estimated and true HR values in the i-th time window in BPM, computed from PPG and ECG windows respectively as in (1):

$$AE_i = |HR_{est}(i) - HR_{true}(i)| \tag{1}$$

Other common metrics widely used-Average Absolute Error (AAE), Standard Deviation of the Absolute Error (SAE) and Average Relative Error (ARE) [14], computed as in (3–5), where N is the total number of estimates (number of windows). Bland-Altman plots and Pearson's correlation coefficient are also widely used to assess the similarity (limit of agreement) between HR_{est} and HR_{true}. These error metrics have been widely reported in state-of-the-art methodologies.

$$AAE = \frac{1}{N}\sum_{i=1}^{N} AE_i \tag{2}$$

$$SAE = \sqrt{\frac{1}{N}\sum_{i=1}^{N} (AE_i - AAE)^2} \tag{3}$$

$$ARE = \frac{1}{N}\sum_{i=1}^{N} \frac{AE_i}{HR_{true}(i)} \tag{4}$$

B. Algorithms Evaluated on SPC Database

Algorithms for HR estimation from wrist-worn PPG, generally comprise four key steps. First, pre-processing the signal, which involves band-pass filtering, downsampling and/or normalizing to zero mean-unit variance. Second, MA removal, using techniques highlighted in Section III (A), in association with a motion reference signal. Third, HR estimation by analyzing the spectral component of the clean signal. Finally, a post-processing stage which takes the form of a tracking algorithm and ensures that HR predictions of consecutive windows do not differ more than a threshold, in agreement with the physiology. Most algorithms in recent literature, essentially adhere to these four steps, differing in employed techniques and associated parameters.

Developments on HR estimation from wrist-worn PPG illuminated with green light, has been mainly propagated by the three-stage TROIKA method, based on signal decomposition, sparsity-based high-resolution spectrum estimation, spectral peak tracking and verification [16]. The signal decomposition is aimed at removing the overlapping (frequency band) MA component from cardiac component. It further helps to sparsify the PPG spectra facilitating the sparsity-based high-resolution spectrum estimation. The spectral peak tracking with verification helps to select the correct spectral peaks corresponding to HR. An AAE of 2.34 BPM was reported on PPG recordings of 12 subjects from the SPC database.

TROIKA was enhanced by JOSS [27], employing joint (PPG and acceleration signals) spectral estimation using a common sparsity constraint on spectral coefficients, achieved by means of a multiple measurement vector (MMV) model [50]. The PPG spectra is cleansed by comparing the spectral coefficients with the acceleration spectra at the same frequency bins, thereby negating the requirements for signal decomposition, temporal difference operations, spectral peak tracking and verification steps as in TROIKA. The error was reduced to 1.28 BPM when evaluated on the same 12 subjects. However, both these successful methods-TROIKA and JOSS rely on large matrices/parameters which poses a challenge for embedded implementations. Furthermore, the accuracy of HR tracking in TROIKA depends on the robustness of initial estimates.

A multiple spectral peak tracking method was reported in [51], using Window's Adaptive Noise Cancellation (ANC), to remove in-band motion disturbances in the PPG signal. The HR is estimated from the denoised signal by Spectral Peak Tracking (SPT) similar to [16]. A novel multi-initialization scheme is used unlike single initialization in [16] and hence the approach is referred as multiple initialization based SPT (MISPT), in which multiple estimated HR trajectories are combined using trajectory strength. An average error of 1.26 ± 2.90 (AAE ± SAE) was reported on 12 SPC subjects. Following these three studies [16] [27] [51], a host of other spectral estimation and decomposition methods were applied on PPG and acceleration signals which reported lower errors, some of the significant one's, using different techniques have been described here.

Clean PPG signal reconstruction using time-varying spectral analysis was presented in [45], termed as SpaMA comprising five distinct stages: time-varying power spectral density (PSD) calculation, spectral filtering, MA detection, HR reconstruction and signal reconstruction. A window-segmented PSD of both PPG and accelerometer signals is calculated, to scale each PSD estimate by the equivalent noise bandwidth of the window. The algorithm compares the first three computed peaks and corresponding frequencies of the PPG spectrum to the first peak and frequency of the acceleration spectra at each window and, the frequency components that are different from the accelerometer frequency are chosen, discarding the coherent peaks (signifying MA in the PPG signal). By reconstructing the HR frequency at each window, simultaneously the PPG signal is reconstructed by using the power, frequency and phase of the signal that corresponds to the HR frequency. The average estimation errors are 0.89, 1.93 and 18 BPM when evaluated on the SPC training, testing and Chon Lab datasets, respectively, with an overall error of 1.86 BPM, reported on all 33 subjects.

An algorithm proposed in [37] uses Singular Value Decomposition (SVD), to decompose the acceleration data into periodic MA components. Since, acceleration data are convoluted noisy signals, using them directly as MA reference [52] would affect convergence of the subsequently applied adaptive filter, resulting in degraded performance. These components are then suppressed in the PPG signals by adaptive filtering yielding clean PPG with sparse spectrum. It is followed by a spectral analysis step applying a few iterations of the Iterative Method with Adaptive Thresholding (IMAT) sparse reconstruction algorithm [53] to achieve a higher resolution spectrum of the cleansed signals and selects the spectral peaks corresponding to HR. Results on 12 subjects of SPC database show an AAE of 1.25 BPM.

A two-stage novel technique is presented in [28], relying on an ensemble empirical mode decomposition (EEMD) for signal denoising together with an *absolute criterion*(AC) which prevents it from depending on previous HR estimates. The second stage, increases the algorithm's robustness against off-track errors by using recursive least squares filters complemented with time-domain extraction. The algorithm produces an AAE of 1.02 ± 1.79 BPM for 12 SPC subjects. Different from all previously mentioned techniques, a joint framework, named as Short-time Fourier Spectral Tracking (SFST) for HR monitoring has been proposed in [54]. It demonstrates that adopting acceleration signals for spectral subtraction from PPG, does not show added advantage over the proposed method. The methodology evaluated on 12 SPC subjects produces an AAE of 1.06 ± 0.69 BPM.

Continuing with the success of using adaptive filters, a hybrid approach combining second-order RLS Volterra filter and TROIKA [16] were proposed in [55]. A custom binary decision block decides on using singular spectrum analysis (SSA) decomposition depending on the correlation between the filtered PPG and acceleration signals. Spectral peak tracking and verification is used to estimate HR, achieving 1.16 BPM and 2.98 BPM on the training/testing SPC database, respectively. The method was also evaluated on 8 extra datasets, acquired similarly as [16], with subjects performing non-rhythmic movements, such as cooking and dancing. An average error of 7.5 BPM was reported over 8 subjects, however, evaluating without the decision block (i.e. only RLS+SSA), results in lower average error of 7.05 BPM. RLS filters were also used by the framework, MURAD [56], based on adaptive noise cancellation with four reference signals, namely, three-axis acceleration and difference between two PPG channels. Probable HR values are estimated from the MA-free PPG outputs of the four RLS filters. A heuristic peak verification technique produces low MAE errors of 0.97 ± 1.82 BPM and 2.25 ± 4.32 BPM on the training/test SPC datasets. A multi-stage cascaded RLS adaptive filter in conjunction with SSA is used in [57], using the three axis acceleration as reference for each filter block for removing MA. A weighted moving average tracking is used for HR estimation, achieving an error of 1.16 ± 1.74 BPM on 12 SPC subjects. Another method involving three-stages of spectrogram normalization (with median filtering and adaptive thresholding), followed by spectrogram conditioning using dynamic time warping and lastly a spectral masking technique successfully estimates HR from PPG [58]. It produces a MAE 1.07 on 12 SPC subjects.

The developments reported in [16], [27], [28], [37], [45], [55]–[59], are usually accompanied with increased number of free parameters, leading to overfitting since they were evaluated on fixed size dataset. Further, the use of recursive adaptive filtering, is computationally intensive for embedded implementation for real-time operation. A Wiener filter and phase vocoder based approach [14] was adopted to attenuate the noise (estimated from accelerometers) in the PPG signal. The phase vocoder helps to overcome the limited resolution of discrete Fourier transform and refine the initial dominant frequency estimation. A user-adaptive post-processing step is introduced and additionally an offline Viterbi decoding post-processing is proposed, devoid of tunable parameters. The results are comparable to state-of-the-art methodologies, reporting an AAE of 1.02 BPM on 12 subjects and an overall AAE of 1.90 on all 23 SPC records.

C. Algorithms Targeting Low-Computational Complexity

In recent developments, low-complexity processing has gained prominence with an eye on real-time HR estimation in resource constrained sensor nodes. A methodology using Fast Fourier transform (FFT) spectrum of short windows of PPG and tri-axial accelerometer signals, was proposed in [19]. It achieves an AAE of 1.27 ± 0.91 BPM on 12 SPC subjects and executes in 226 ms on a wearable PPG device, obtaining a battery lifetime of approximately 9 days.

A computationally efficient technique based on adaptive NLMS filters was proposed in [60]. The output of six filters (tri-axial acceleration and 2-channel PPG) are combined into a single enhanced time-frequency domain representation, enabling HR estimation. The approach, evaluated in real-time, produced an AAE of 1.77 ± 1.20 BPM on 12 SPC subjects. As a follow up, [61] has proposed avoiding the NLMS filters, by applying correlation functions to enhance periodic components (from acceleration spectra) and suppress wideband noise caused by MA. The HR estimator finds the maximal value in a weighted spectrum using linear prediction, achieving an AAE of 1.32 ± 1.24 BPM. The key achievement lies in the computation time of 3.73 seconds, approximately 80 times faster than JOSS [27] and 14 times faster than [60].

The best results on the SPC database are reported by a recent study [62], where the PPG signal is initially cleaned using the accelerometer spectrum through Wiener filtering, similar to [14]. The study highlights the limitations of currently used post-processing techniques, which are mainly based on history tracking. The error in HR values obtained from clean PPG at each window, is analyzed in conjunction with a custom metric known as Crest factor (CF). CF is shown to be inversely related to the HR error and acts as a signal quality indicator for each PPG window. The post-processing involves using a finite state machine (FSM) to toggle between four custom defined states–*stable*, *recovery, alert* and *uncertain*, triggered by the CF and HR changes. HR computed every 2 s, on 8 s windows, shows the efficacy of the method, reporting an error of 0.99 BPM on 23 SPC subjects. The study most importantly highlights the shortcomings of the accelerometer data for MA removal. Acceleration is unable to represent MA corresponding to fine-grain finger/wrist movements/gestures and hence might exhibit an uncorrelated behavior with MA. Furthermore, dominant accelerometer frequencies might overlap with true HR frequencies. Hence, the authors follow up with a new study [63] using gyroscope. PPG, acceleration and gyroscope signals were downsampled to 25 Hz and a 2048 point FFT was computed to clean the PPG signal using power spectral filtering. HR was computed by combining the FSM method [62] with a Direct Finding of the Dominant Frequency (DFDF) approach over the range 0.6–3.3 Hz. Experiments were performed with 24 participants (10 male and 14 female), collecting data with a custom wrist watch at 50 Hz, while walking and running (6 to 7 km/h) on a treadmill. The results demonstrate that during walking, the gyroscope estimates HR better in comparison to an accelerometer, whereas during running the difference is marginal. A gyroscope consumes more power as compared to an accelerometer, hence it is advised to switch between the two sensors depending on the motion situation.

However, both a gyroscope and an accelerometer are incompetent to track micro-motions involving the finger (e.g. tapping) and the wrist (e.g. fist opening/closing). Hence, a recent study [64] proposes using an optic motion reference for MA cancellation. This helps to reduce the form factor of the device by ignoring the need for an accelerometer. The green light is used for HR estimation, while the IR signal is used as motion reference. The framework uses a continuous wavelet transform based motion removal step followed by HR estimation and signal reconstruction. The algorithm produces low AAE values when tested on 21 types of motion from 6 healthy subjects. However, it needs to be verified on intense physical activities.

D. Learning Based Algorithms

Moving away from traditional techniques, a supervised learning approach was proposed in [15], to detect heart beats at each position of a PPG signal. From a training set of labeled PPG segments, a set of features is extracted to classify beat vs inter-beat samples, allowing reliable HR estimation through lightweight postprocessing. Random Forest was the best classifier compared to Linear discriminant (LDA), Quadratic discriminant, 5-nearest neighbors and 10-nearest neighbors.

A neural network framework proposed in [65] successfully estimates HR, with an error of 1.39 BPM and 2.81 BPM, when evaluated on 12 and all 23 subjects, respectively. A candidate peak selection is performed on the pre-processed PPG signals, assigning a probability to each spectral peak which can correspond to a HR peak, followed by feature extraction, selection and a 3-layer multi-layer perceptron (MLP) network with 22 neurons [65]. An approach based on Internet of Things (IoT) was adopted, using cloud connectivity of smartphones for selection of PPG signals. The pre-processed PPG signal was used to extract 11 time-domain features and then clustered into different groups based on motion and physiology of the subjects. A three layer deep belief network was trained using Restricted Boltzmann Machines on 2s PPG signals, producing an error of 4.8% on the SPC training database [66].

Lastly, a Deep learning framework, *CorNET* [67], using convolutional neural network (CNN) and long-short term memory (LSTM) was evaluated on SPC database to predict HR from PPG signals. The supervised learning framework, negates the need for manual feature extraction. It achieves an AAE of 1.47±3.37 BPM for 22 SPC subjects and was also successfully evaluated on custom data from 2 subjects performing daily activities. Although promising, these early

TABLE II
SUMMARY OF STATE-OF-THE-ART SIGNAL PROCESSING TECHNIQUES FOR HR ESTIMATION FROM WRIST PPG SPC DATASET

Ref	Algorithm	Signals	Pre-processing	Post-processing	Results	Complex
[16]	Signal decomposition for denoising, sparse signal reconstruction for high-resolution spectrum estimation, and spectral peak tracking (TROIKA)	PPG; acceleration	2nd order bandpass filter (0.4 - 5 Hz); Signal downsampled to 25 Hz	Thresholding, history tracking	2.42 BPM on 12 subjects	H
[27]	Multiple measurement vector (MMV) model for joint sparse signal recovery, exploiting the common spectral structures between PPG and acceleration signals. The frequency bins of MA in PPG spectrum are removed through spectral subtraction on the reconstructed spectrum.	PPG; acceleration	2nd order bandpass filter (0.4 - 4 Hz); Signal downsampled to 25 Hz	Similar to [16]	1.28 BPM on 12 subjects	H
[51]	Window's adaptive noise cancellation (ANC) is used to remove in-band motion from PPG. HR is estimated from denoised PPG using a multi-initialization based spectral peak tracking (SPT) algorithm as opposed to single initialization in [16] and trigger-driven initialization scheme in [19].	PPG	N/A	N/A	1.28 BPM on 12 subjects	H
[14]	Novel algorithm (WFPV) using Wiener filtering to attenuate MA in PPG using noise signatures from acceleration followed by a phase vocoder for refining HR estimates and an adaptive post-processing step.	PPG; acceleration	4th order bandpass filter (0.4 - 4 Hz); z-score normalisation and averaged; downsampled to 25 Hz	Thresholding, history tracking	1.02, 1.97 BPM on 12 and 23 subjects	L
[45]	Spectral filter algorithm for MA and heart rate reconstruction (SpaMA) – based on power spectral density estimation of both PPG and acceleration.	PPG; acceleration	bandpass filter (0.5 - 3 Hz); downsampled to 31.25 Hz	History tracking and cubic spline interpolation	0.89, 3.36 BPM on 12, 13-23 subjects	H
[62]	PPG is cleaned using Winer filtering w.r.t acceleration spectrum. Post-processing is done using a novel Finite state machine (FSM), where the transitions are triggered by changes in custom metric – 'Crest Factor (CF)'.	PPG; acceleration	4th order Butterworth band pass filter (0.4-4 Hz); z-score normalisation and averaged; downsampled to 25 Hz.	FSM triggered by CF	0.99 BPM on 23 subjects	L
[37]	MA cancellation by SVD decomposing of the acceleration into periodic components, suppressed by adaptive filtering. A Spectral Analysis step applies a few iterations of the IMAT (Iterative Method with Adaptive Thresholding) sparse reconstruction algorithm [11], [12] to achieve a higher resolution spectrum of the cleansed signals and selects the HR spectral peaks.	PPG; acceleration	bandpass filter (0.4 – 5 Hz)	Peak selection and thresholding	1.25 BPM on 12 subjects	H
[28]	Noise-assisted EEMD technique together with an absolute criterion (AC), employed to negate dependency on previous HR estimates. Additionally, RLS filters complemented with time-domain extraction is used to refine the HR values.	PPG; acceleration	Bandpass filter to 40-100 BPM; downsampled to 25 Hz	Peak tracking and thresholding	1.02 BPM on 12 subjects	H
[54]	Joint framework combining STFT and spectral analysis (detection, verification and predication) is adopted to predict HR in real-time.	PPG	zero-phase forward and reverse digital IIR filter	cyclic moving average filter	1.06 BPM on 12 subjects	H
[67]	*CorNET* – ECG-assisted supervised learning framework, using deep learning – 2-layer CNN, 2-layer LSTM and fully connected layer.	PPG	4th order Butterworth band pass filter (0.4-18 Hz); z-score normalisation, using one PPG channel only.	N/A	1.47 BPM on 22 subjects	H

developments would require comprehensive exploration for embedded implementation aimed at real-time operations, given the complexity involved in feature engineering and high number of training parameters.

The list of unique processing techniques, along with evaluation results on SPC and other databases has been summarized in Tables II and III, respectively. We denote the complexity of the reviewed methods in the tables as high (H) or

TABLE III
HR ESTIMATION FROM WRIST PPG–METHODS EVALUATED ON OTHER DATABASES

Ref	Algorithm	Signals	Pre-processing	Post-processing	Results	Complex
[63]	Spectral subtraction to remove MA from PPG, but using gyroscope data instead of acceleration. HR was computed with a DFDF (direct finding the dominant frequency) approach which finds the dominant frequency and followed by the FSM method [62].	PPG; gyroscope; acceleration	band pass filter (0.4-4 Hz); z-score normalisation and averaged; downsampled to 25 Hz.	FSM triggered by CF	Walking: 1.92 BPM; running: 1.60 BPM on 24 subjects	L
[67]	*CorNET* – ECG-assisted supervised learning framework, using deep learning – 2-layer CNN, 2-layer LSTM and fully connected layer.	PPG	4th order Butterworth band pass filter (0.4-18 Hz); z-score normalisation, using one PPG channel only.	N/A	7.2 BPM on 2 subjects (*IMEC-Db*)	H
[55]	Hybrid approach combining, second order RLS Volterra filter, custom binary decision block and SSA-based signal decomposition, in association with spectral peak tracking and verification.	PPG; acceleration	Bandpass filter to 0.4 – 5 Hz. 40-100 BPM;	Peak tracking and thresholding	7.5 BPM on 8 subjects	H

low (L) with respect to feasibility of real-time processing. The complexity is based on the average simulation time per window (ASTPW) [58], computed for various methods.

E. Commercial Devices

The growing market on wearable health monitors has propelled innovation in physiological data acquisition and is worth millions of dollars [64]. The utility of the products, from optimizing athletic performance to providing real-time clinical grade data, act as a driver in generating low-cost pervasive solutions [65]. Currently, there are several smart watches with PPG sensors. A review [66] compares the accuracy of 6 popular commercially available devices: Scosche Rhythm (SR), Mio Alpha (MA), Fitbit Charge HR (FH), Basis Peak (BP), Microsoft Band (MB), and the TomTom Runner Cardio (TT). The wrist-worn PPG HR is computed for a 30 minute protocol divided into 5 minute phases, including walking and running at five different speeds, and compared to a Polar RS400 HR chest strap, considered to be robust to MA. The minimum absolute mean error percentage difference ranged from 3.3% to 6.2%. The average correlation of all six devices with the Polar chest strap was reported at 0.94. These devices are all highly tuned and rely on post-processing algorithms to achieve respectable numbers. Fitbit utilizes a solution that toggles the HR algorithm between resting and activity levels of the user, by additionally monitoring acceleration as mentioned in [67]. The popular Apple Watch leverages multiple LEDs configured parallel to the blood vessel to measure the time difference as the blood pulse moves across the sensors to estimate external noise or MA [69].

A recent study [68] also compared commercial wrist-worn HR monitors, over a range of exercise intensities (cycling), with controlled upper body movement. They used an Apple watch Series 1, Fitbit Charge, TomTom Touch, Mio Fuse, Polar S610i chest belt, 5-lead Vyntus ECG system for reference. Experiments conducted on 18 healthy subjects (16 male, 2 female), reveal that HR readings of the Vyntus ECG and Polar chest strap never differed by more than 5 BPM during the experiment. During exercise, the Apple watch differed by 2.2%, Mio by 4.4%, Tomtom by 11.1% and Fitbit 21.1% from the reference. .During a recovery phase after exercise, the Apple watch differed by 27.8%, Mio 11.1%,Tomtom 16.7% and Fitbit 11.1% from the reference. In general, the study reveals the effectiveness of chest worn HR monitors over wrist worn devices. The increased HR error in the recovery period raises concerns over the sensitivity of the devices to fast changes in HR. Only the Fitbit and Tomtom devices show significant effect of exercise intensity on the errors, which is connected to lower blood perfusion at low HR. The Apple watch and the MioFuse produce most valid outputs.

Another study [69], aimed at estimating the accuracy of wrist-worn activity trackers during controlled and ambulant environment, used a Fitbit Charge and MioFuse, both having tri-axial acceleration and PPG. Alongside, a NL-1000 accelerometer was used on waistband for activity reference and a Polar T31 chest belt for ECG reference. Experiments conducted on 40 participants, show that accuracy for step detection and energy expenditure increases with exercise intensity, however the HR accuracy drops. The effectiveness of using wrist-worn HR data in addition to acceleration for activity recognition was investigated in [70]. The study concludes, that using a Random Forest classifier in conjunction with time/frequency features, proved effective in classifying high intensity cycling considering both HR and acceleration information, whereas sitting, standing and cleaning could be detected only with acceleration features. These studies [68]–[70], used proprietary software for estimating HR. To the best of knowledge, none of the referred commercial sensors, provide access to raw PPG data. This highlights the need for development of a raw, unprocessed PPG database incorporating wrist-worn signals with wide variability in subject physiology, facilitating future research.

F. HRV Estimation

Moving away from the primary focus on average HR estimation, some initial work has been reported on HRV measurements. Given a fixed average HR, the time between each individual heart beat may not be constant, since it is actively modulated by the Autonomic Nervous System. This gives rise to HR variability, characterized by a range of time and frequency domain parameters. Instantaneous Heart Rate (IHR) is an important measurement in this context, since it is based on the time interval between consecutive R-peaks in the ECG trace. HRV can be seen as a bio-marker of autonomic activity (myocardial infarction and diabetic neuropathy, etc), carrying significant clinical interest [71]–[74]. The feasibility of using pulse rate variability (PRV), estimated from PPG signals, as an alternative to HRV has been well explored in literature. The main difference between these values is the time taken by the pulse to travel from the heart to the arm, referred as pulse transit time (PTT), varying with posture and blood pressure. Studies performed in stationary conditions using time-invariant analysis showed that PRV is a good surrogate of HRV [75].

Average HR estimation has usually been calculated every 2s using an 8s sliding window of PPG data [16], [27], [28], [37], [45], [59], causing the loss of instantaneous information. Nonetheless, MA poses a challenge in extracting IHR, especially in ambulant conditions. A recent study has reported a novel MA removal technique facilitating IHR estimation [18]. The outcomes are compared against a novel IHR algorithm on ECG. The algorithms for both PPG and ECG are based on instantaneous spectral measures calculated using EMD and Hilbert Transform with a novel spectral masking stage. The algorithms differ in the pre- and post-processing stages, wherein for ECG the pre-processing is performed to extract an initial estimate of R-peak locations, and post-processing is performed using a particle filter. For PPG, pre-processing is performed using a bank of adaptive filters without a post-processing stage. The IHR variance over a 40s data segment extracted during motion is estimated correctly to within 1.75 BPM for PPG and within 0.27 BPM for ECG signals.

IV. Further Applications of Wrist-PPG

Early work reported on biometric identification and disease management, have been briefly discussed in this section.

A. Biometric Identification

Biometrics as defined by the International Organization for Standardization (ISO) is the "automated recognition of individuals based on their behavioral and biological characteristics" where common biological characteristics used are fingerprints, iris, DNA, voice and gait analysis [76]. Recent studies on biometrics have also focused on one-dimensional physiological signals, i.e. ECG [77], electroencephalogram (EEG) [78], phonocardiogram (PCG) and lastly PPG [79], [80]. Such physiological signals have the distinct advantage of enabling continuous authentication systems, since they can be captured for long time periods. PPG-based biometric identification has been a popular research topic, but of them have used PPG collected in clinical settings, thereby making these models unsuitable for ambulatory usage [80].

Earlier efforts on PPG-based identification have focused on data collected from the finger and analyzed using frequency spectrum (Fourier analysis), correlation, peaks, feature extraction and classification employing fuzzy-logic [79], [80] and LDA [81], yielding accuracies of 90-95%. Furthermore, learning based approaches have relied on hand crafted features, using up to 40 features in conjunction with a k-NN classifier [82]. A recent work has focused on a two-stage procedure involving clustering (on 11 features) and RBM-DBN, evaluated on 12 SPC subjects [83]. Also, *CorNET*, achieves an accuracy of 96% on 20 SPC subjects [67]. Results are promising, which paves the way for future research to deploy systems to perform model update based on the changing physiology of the subjects and to implement hardware-based security, which are yet to be explored on a system level.

B. Disease Diagnosis Using Wrist-PPG

Atrial Fibrillation (AF), is the most common cardiac arrhythmia in clinical practice affecting millions of people [84]–[86]. This underscores the need for an affordable, continuous and portable AF monitoring system, allowing early diagnosis and treatment. Although ECG has been the preferred modality for AF detection, alternate solutions based on smartphone sensors have surfaced due to their ubiquitous nature [87]. These sensors capture PPG data from the finger tip of patients and accurately discriminate AF from normal sinus rhythm (SR) and premature beats, and increase patient compliance related to the ease of use, however fall short of capturing transient or asymptomatic AF.

A recent work by Philips research highlighted AF detection using wrist PPG by determining the timing of heartbeats and inter-beat interval (IBI) [88]. Acceleration and PPG morphology were used to discard IBIs in presence of motion artifacts. A first-order Markov Model validated on ECG signals was used to assess the probability of irregular rhythms due to AF using PPG-derived IBIs and to classify absence of AF in patients showing sporadic premature beats. AF detection was achieved with 97 $\pm$ 2% sensitivity and 99 $\pm$ 3% specificity. However, the data used is not publicly available. Another recent study focused on classification of AF versus SR by means of extracting RR intervals by detecting systolic downstrokes of wrist-worn, infrared PPG waveforms [89]. Classification was performed using time domain features in conjunction with support vector machine, achieves an accuracy of 93.85%. Furthermore, a novel wavelet and CNN based approach was proposed to classify AF from wrist-worn multichannel PPG signals [90]. A continuous wavelet transform was applied to PPG and then a CNN was trained on the spectrograms to detect AF. Combining the output of CNN with features calculated based on beat-to-beat variability and signal quality provided a significant discriminatory power. This yielded cross-validation accuracy of 91.8% and Area Under the Curve of 0.95, comparable to state-of-the-art ECG-based AF detection approaches on ambulatory data.

V. Conclusion

In this paper, we have presented a comprehensive review on wrist-worn PPG sensors used in ambulatory environment, encompassing state-of-the-art research work and open avenues presenting potential for future development. Increased CVD risks and associated expenditures, have enabled technological development towards ubiquitous health monitoring. There is a major research drive to move from a multi-sensor monitoring modality to single sensor based daily life monitoring especially among the healthy population, aiding pervasive heath management. This article presents details on sensing modality and algorithm development for wrist-worn PPG, facilitating vital parameter estimation targeting key applications. Although successful research initiatives have been reported and there is an abundance of commercial devices using wrist PPG sensors, it is important to focus on the fundamental problem of MA removal. Varying degrees of MA, as highlighted in [63]–[64] are not well captured by the accelerometer and hence detailed research into alternate motion references (e.g. gyroscope, photoelectric, pressure sensors, etc.), need to be performed. Maintaining a constant pressure between the photosensor and skin surface, minimizing the displacement for long duration monitoring, sweat in the stratum corneum affecting the reflectance-PPG measurement mechanism, are factors which require a close cooperation between hardware and algorithm development. Solving these issues could lead to wrist PPG being used for longitudinal clinical monitoring and make it effective for various applications.

It would be beneficial for future research initiatives to focus on–a) development of publicly available database, in addition to [17], [92], [63], incorporating a wide variability of healthy and CVD subjects; b) light-weight algorithms which can be embedded into resource constrained wrist-worn sensor platform; c) developing off-the-shelf (COTS) sensor modules, facilitating collection of raw PPG data with archetypal experiments; d) clinical validation guidelines and documentation for wrist-PPG parameters; e) development of novel signal quality indicators [93] which would in effect aid the fidelity of vital parameter estimation; f) measuring arterial blood oxygen saturation (SpO2) on the wrist (measured normally from the finger), a vital cardiac parameter indicating the levels of blood oxygenation [94]. We believe the technological advancements although at a nascent stage, have potential to grow at a rapid pace enabling pervasive CVD monitoring.

Acknowledgment

The authors would like to acknowledge the help of Luke Everson (University of Minnesota, Minnesota, USA, email: evers193 @umn.edu) and Mario Konijnenburg (Holst Centre, Eindhoven, Netherlands, e-mail: Mario.Konijnenburg@ imec-nl), toward this manuscript.

References

[1] T. Rault, A. Bouabdallah, Y. Challal, and F. Marin, "A survey of energy-efficient context recognition systems using wearable sensors for healthcare applications," *Pervasive Mobile Comput.*, vol. 37, pp. 23–44, Jun. 2017.

[2] S. M. Riazul Islam, D. Kwak, M. Humaun Kabir, M. Hossain, and K.-S. Kwak, "The Internet of Things for health care: A comprehensive survey," *IEEE Access*, vol. 3, pp. 678–708, 2015.

[3] B.-S. Lin, A. M. Wong, and K. C. Tseng, "Community-based ECG monitoring system for patients with cardiovascular diseases," *J. Med. Syst.*, vol. 40, no. 4, p. 80, Apr. 2016.

[4] D. G. Benditt, W. O. Adkisson, R. S. Sutton, R. K. Mears, and S. Sakaguchi, "Ambulatory diagnostic ECG monitoring for syncope and collapse: An assessment of clinical practice in the United States," *Pacing Clin. Electrophysiol.*, vol. 41, no. 2, pp. 203–209, 2018.

[5] M. K. Kharde *et al.*, "Low cost ECG monitoring system for the patient using smart device: Design and implementation," *Imperial J. Interdiscipl. Res.*, vol. 3, no. 12, pp. 80–84, 2017. [Online]. Available: https://www.onlinejournal.in/IJIRV3I12/014.pdf

[6] A. Khushhal *et al.*, "Validity and reliability of the apple watch for measuring heart rate during exercise," *Sports Med. Int. Open*, vol. 1, no. 6, pp. E206–E211, 2017.

[7] K. M. Diaz *et al.*, "Fitbit: An accurate and reliable device for wireless physical activity tracking," *Int. J. Cardiol.*, vol. 185, pp. 138–140, Apr. 2015.

[8] S. E. Kirk *et al.*, "Comparison of the apple watch, fitbit surge, and actigraph GT9X link in measuring energy expenditure, steps, distance, and heart rate," College Educ. Human Services, Cleveland State Univ., Cleveland, OH, USA, Tech. Rep, 2016. [Online]. Available: https://etd.ohiolink.edu/!etd.send_file?accession=csu1462375247&disposition=inline

[9] S. K. Vashist, E. M. Schneider, and J. H. T. Luong, "Commercial smartphone-based devices and smart applications for personalized healthcare monitoring and management," *Diagnostics*, vol. 4, no. 3, pp. 104–128, 2014.

[10] D. Phan, L. Y. Siong, P. N. Pathirana, and A. Seneviratne, "Smartwatch: Performance evaluation for long-term heart rate monitoring," in *Proc. Int. Symp. Bioelectron. Bioinformat. (ISBB)*, Oct. 2015, pp. 144–147.

[11] J. Allen, "Photoplethysmography and its application in clinical physiological measurement," *Physiol. Meas.*, vol. 28, no. 3, p. R1, Feb. 2007.

[12] A. Kamal, J. B. Harness, G. Irving, and A. J. Mearns, "Skin photoplethysmography—A review," *Comput. Methods Programs Biomed.*, vol. 28, no. 4, pp. 257–269, Apr. 1989.

[13] T. Aoyagi and K. Miyasaka, "Pulse oximetry: Its invention, contribution to medicine, and future tasks," *Anesthesia Analgesia*, vol. 94, no. 1, pp. S1–S3, 2002.

[14] A. Temko, "Accurate heart rate monitoring during physical exercises using PPG," *IEEE Trans. Biomed. Eng.*, vol. 64, no. 9, pp. 2016–2024, Sep. 2017.

[15] E. Grisan *et al.*, "A supervised learning approach for the robust detection of heart beat in plethysmographic data," in *Proc. 37th Annu. Int. Conf. IEEE Eng. Med. Biol. Soc. (EMBC)*, Aug. 2015, pp. 5825–5828.

[16] Z. Zhang, Z. Pi, and B. Liu, "TROIKA: A general framework for heart rate monitoring using wrist-type photoplethysmographic signals during intensive physical exercise," *IEEE Trans. Biomed. Eng.*, vol. 62, no. 2, pp. 522–531, Feb. 2015.

[17] (2015). *IEEE SPC*. Accessed: Feb. 5, 2017. [Online]. Available: https://sites.google.com/site/researchbyzhang/ieeespcup2015

[18] D. Jarchi and A. J. Casson, "Towards photoplethysmography-based estimation of instantaneous heart rate during physical activity," *IEEE Trans. Biomed. Eng.*, vol. 64, no. 9, pp. 2042–2053, Sep. 2017.

[19] E. de Giovanni, S. Murali, F. Rincon, and D. Atienza, "Ultra-low power estimation of heart rate under physical activity using a wearable photoplethysmographic system," in *Proc. Euromicro Conf. Digital Syst. Design (DSD)*, Sep. 2016, pp. 553–560.

[20] O. Faust, U. R. Acharya, E. Y. N. Ng, and H. Fujita, "A review of ECG-based diagnosis support systems for obstructive sleep apnea," *J. Mech. Med. Biol.*, vol. 16, no. 1, 2016, Art. no. 1640004.

[21] M. Merone, P. Soda, M. Sansone, and C. Sansone, "ECG databases for biometric systems: A systematic review," *Expert Syst. Appl.*, vol. 67, pp. 189–202, Jan. 2017.

[22] P. Melillo, R. Castaldo, G. Sannino, A. Orrico, G. de Pietro, and L. Pecchia, "Wearable technology and ECG processing for fall risk assessment, prevention and detection," in *Proc. 37th Annu. Int. Conf. IEEE Eng. Med. Biol. Soc. (EMBC)*, Aug. 2015, pp. 7740–7743.

[23] R. Gupta, *ECG Acquisition and Automated Remote Processing*. New York, NY, USA: Springer, 2016.

[24] T. Tamura, Y. Maeda, M. Sekine, and M. Yoshida, "Wearable photoplethysmographic sensors—Past and present," *Electronics*, vol. 3, no. 2, pp. 282–302, 2014.

[25] Y. K. Lee, J. Jo, and H. S. Shin, "Development and evaluation of a wristwatch-type photoplethysmography array sensor module," *IEEE Sensors J.*, vol. 13, no. 5, pp. 1459–1463, May 2013.

[26] V. Vizbara, "Comparison of green blue and infrared light in wrist and forehead photoplethysmography," in *Proc. 17th Int. Conf. Biomed. Eng.*, 2013, vol. 17, no. 1, pp. 78–81.

[27] Z. Zhang, "Photoplethysmography-based heart rate monitoring in physical activities via joint sparse spectrum reconstruction," *IEEE Trans. Biomed. Eng.*, vol. 62, no. 8, pp. 1902–1910, Aug. 2015.

[28] E. Khan, F. Al Hossain, S. Z. Uddin, S. K. Alam, and M. K. Hasan, "A robust heart rate monitoring scheme using photoplethysmographic signals corrupted by intense motion artifacts," *IEEE Trans. Biomed. Eng.*, vol. 63, no. 3, pp. 550–562, Mar. 2016.
[29] D. Li, H. Zhao, and S. Dou, "A new signal decomposition to estimate breathing rate and heart rate from photoplethysmography signal," *Biomed. Signal Process. Control*, vol. 19, pp. 89–95, May 2015.
[30] A. B. Hertzman, "Observations on the finger volume pulse recorded photoelectrically," *AmER. J. Physiol.*, vol. 119, pp. 334–335, Sep. 1937.
[31] J. G. Webster, *Design of Pulse Oximeters*. Boca Raton, FL, USA: CRC Press, 1997.
[32] R. R. Anderson and J. A. Parrish, "The optics of human skin," *J. Investigative Dermatol.*, vol. 77, no. 1, pp. 13–19, Jul. 1981.
[33] Y. Maeda, M. Sekine, and T. Tamura, "The advantages of wearable green reflected photoplethysmography," *J. Med. Syst*, vol. 35, pp. 829–834, Oct. 2011.
[34] Y. Sun and N. Thakor, "Photoplethysmography revisited: From contact to noncontact, from point to imaging," *IEEE Trans. Biomed. Eng.*, vol. 63, no. 3, pp. 463–477, Mar. 2016.
[35] D. Jarchi and A. J. Casson, "Description of a database containing wrist PPG signals recorded during physical exercise with both accelerometer and gyroscope measures of motion," *Data*, vol. 2, no. 1, p. 1, Dec. 2016.
[36] R. Yousefi, M. Nourani, S. Ostadabbas, and I. Panahi, "A motion-tolerant adaptive algorithm for wearable photoplethysmographic biosensors," *IEEE J. Biomed. Health Informat.*, vol. 18, no. 2, pp. 670–681, Mar. 2014.
[37] M. B. Mashhadi, E. Asadi, M. Eskandari, S. Kiani, and F. Marvasti, "Heart rate tracking using wrist-type photoplethysmographic (PPG) signals during physical exercise with simultaneous accelerometry," *IEEE Signal Process. Lett.*, vol. 23, no. 2, pp. 227–231, Feb. 2016.
[38] H. Pan, D. Temel, and G. AlRegib, "HeartBEAT: Heart beat estimation through adaptive tracking," in *Proc. IEEE-EMBS Int. Conf. Biomed. Health Inform. (BHI)*, Feb. 2016, pp. 587–590.
[39] M. R. Ram, K. V. Madhav, E. H. Krishna, N. R. Komalla, and K. A. Reddy, "A novel approach for motion artifact reduction in PPG signals based on AS-LMS adaptive filter," *IEEE Trans. Instrum. Meas.*, vol. 61, no. 5, pp. 1445–1457, May 2012.
[40] B. S. Kim and S. K. Yoo, "Motion artifact reduction in photoplethysmography using independent component analysis," *IEEE Trans. Biomed. Eng.*, vol. 53, no. 3, pp. 566–568, Mar. 2006.
[41] R. Krishnan, B. Natarajan, and S. Warren, "Two-stage approach for detection and reduction of motion artifacts in photoplethysmographic data," *IEEE Trans. Biomed. Eng.*, vol. 57, no. 8, pp. 1867–1876, Aug. 2010.
[42] X. Sun, P. Yang, Y. Li, Z. Gao, and Y. T. Zhang, "Robust heart beat detection from photoplethysmography interlaced with motion artifacts based on empirical mode decomposition," in *Proc. IEEE-EMBS Int. Conf. Biomed. Health Inform.*, Jan. 2012, pp. 775–778.
[43] M. Raghuram, K. V. Madhav, E. H. Krishna, and K. A. Reddy, "Evaluation of wavelets for reduction of motion artifacts in photoplethysmographic signals," in *Proc. 10th Int. Conf. Inf. Sci., Signal Process. Their Appl.*, May 2010, pp. 460–463.
[44] J. Xiong, L. Cai, D. Jiang, H. Song, and X. He, "Spectral matrix decomposition-based motion artifacts removal in multi-channel PPG sensor signals," *IEEE Access*, vol. 4, pp. 3076–3086, 2016.
[45] S. M. A. Salehizadeh, D. Dao, J. Bolkhovsky, C. Cho, Y. Mendelson, and K. H. Chon, "A novel time-varying spectral filtering algorithm for reconstruction of motion artifact corrupted heart rate signals during intense physical activities using a wearable photoplethysmogram sensor," *Sensors*, vol. 16, no. 1, p. 10, 2015.
[46] H. Fukushima, H. Kawanaka, S. Bhuiyan, and K. Oguri, "Estimating heart rate using wrist-type Photoplethysmography and acceleration sensor while running," in *Proc. Annu. Int. Conf. IEEE Eng. Med. Biol. Soc.*, Sep. 2012, pp. 2901–2904.
[47] B. Lee, J. Han, H. J. Baek, J. H. Shin, K. S. Park, and W. J. Yi, "Improved elimination of motion artifacts from a photoplethysmographic signal using a Kalman smoother with simultaneous accelerometry," *Physiol. Meas.*, vol. 31, no. 12, p. 1585, 2010.
[48] J. Yao and S. Warren, "A short study to assess the potential of independent component analysis for motion artifact separation in wearable pulse oximeter signals," in *Proc. IEEE 27th Annu. Conf. Eng. Med. Biol.*, Jan. 2005, pp. 3585–3588.
[49] F. Peng, Z. Zhang, X. Gou, H. Liu, and W. Wang, "Motion artifact removal from photoplethysmographic signals by combining temporally constrained independent component analysis and adaptive filter," *Biomed. Eng. OnLine*, vol. 13, no. 1, p. 50, 2014.
[50] S. F. Cotter, B. D. Rao, K. Engan, and K. Kreutz-Delgado, "Sparse solutions to linear inverse problems with multiple measurement vectors," *IEEE Trans. Signal Process.*, vol. 53, no. 7, pp. 2477–2488, Jul. 2005.
[51] N. K. L. Murthy, P. C. Madhusudana, P. Suresha, V. Periyasamy, and P. K. Ghosh, "Multiple spectral peak tracking for heart rate monitoring from photoplethysmography signal during intensive physical exercise," *IEEE Signal Process. Lett.*, vol. 22, no. 12, pp. 2391–2395, XDec. 2015.
[52] S. H. Kim *et al.*, "Adaptive noise cancellation using accelerometers for the PPG signal from forehead," in *Proc. 29th Annu. Int. Conf. IEEE Eng. Med. Biol. Soc.*, Aug. 2007, pp. 2564–2567.
[53] F. Marvasti *et al.*, "A unified approach to sparse signal processing," *EURASIP J. Adv. Signal Process.*, vol. 2012, p. 44, Feb. 2012.
[54] D. Zhao, Y. Sun, S. Wan, and F. Wang, "SFST: A robust framework for heart rate monitoring from photoplethysmography signals during physical activities," *Biomed. Signal Process. Control*, vol. 33, pp. 316–324, Mar. 2017.
[55] Y. Ye, Y. Cheng, W. He, M. Hou, and Z. Zhang, "Combining nonlinear adaptive filtering and signal decomposition for motion artifact removal in wearable photoplethysmography," *IEEE Sensors J.*, vol. 16, no. 19, pp. 7133–7141, Oct. 2016.
[56] S. S. Chowdhury, R. Hyder, M. S. B. Hafiz, and M. A. Haque, "Real-time robust heart rate estimation from wrist-type PPG signals using multiple reference adaptive noise cancellation," *IEEE J. Biomed. Health Inform.*, vol. 22, no. 2, pp. 450–459, Mar. 2018, doi: 10.1109/JBHI.2016.2632201.
[57] M. T. Islam, I. Zabir, S. T. Ahamed, M. T. Yasar, C. Shahnaz, and S. A. Fattah, "A time-frequency domain approach of heart rate estimation from photoplethysmographic (PPG) signal," *Biomed. Signal Process. Control*, vol. 36, pp. 146–154, Jul. 2017, doi: 10.1016/j.bspc.2017.03.020.
[58] C. Zong and R. Jafari, "Robust heart rate estimation using wrist-based PPG signals in the presence of intense physical activities," in *Proc. 37th Annu. Int. Conf. IEEE Eng. Med. Biol. Soc. (EMBC)*, Aug. 2015, pp. 8078–8082.
[59] B. Sun and Z. Zhang, "Photoplethysmography-based heart rate monitoring using asymmetric least squares spectrum subtraction and Bayesian decision theory," *IEEE Sensors J.*, vol. 15, no. 12, pp. 7161–7168, Dec. 2015.
[60] T. Schäck, C. Sledz, M. Muma, and A. M. Zoubir, "A new method for heart rate monitoring during physical exercise using photoplethysmographic signals," in *Proc. 23rd Eur. Signal Process. Conf. (EUSIPCO)*, Sep. 2015, pp. 2666–2670.
[61] T. Schäck, M. Muma, and A. M. Zoubir, "Computationally efficient heart rate estimation during physical exercise using photoplethysmographic signals," in *Proc. 25th Eur. Signal Process. Conf. (EUSIPCO)*, Sep. 2017, pp. 2478–2481.
[62] H. Chung, H. Lee, and J. Lee, "Finite state machine framework for instantaneous heart rate validation using wearable photoplethysmography during intensive exercise," *IEEE J. Biomed. Health Inform.*, to be published.
[63] H. Lee, H. Chung, and J. Lee, "Motion artifact cancellation in wearable photoplethysmography using gyroscope," *IEEE Sensors J.*, vol. 19, no. 3, pp. 1166–1175, Feb. 2018.
[64] Y. Zhang *et al.*, "Motion artifact reduction for wrist-worn photoplethysmograph sensors based on different wavelengths," *Sensors*, vol. 19, no. 3, p. 673, Feb. 2019.
[65] M. Essalat, M. B. Mashhadi, and F. Marvasti, "Supervised heart rate tracking using wrist-type photoplethysmographic (PPG) signals during physical exercise without simultaneous acceleration signals," in *Proc. IEEE Global Conf. Signal Inf. Process.*, Dec. 2016, pp. 1166–1170.
[66] V. Jindal, "MobileSOFT: U: A deep learning framework to monitor heart rate during intensive physical exercise," Univ. Texas, Dallas, TX, USA, Tech. Rep., 2018. [Online]. Available: https://src.acm.org/binaries/content/assets/src/2016/vasujindal.pdf
[67] D. Biswas *et al.*, "CorNET: Deep learning framework for PPG-based heart rate estimation and biometric identification in ambulant environment," *IEEE Trans. Biomed. Circuits Syst.*, vol. 13, no. 2, pp. 282–291, Apr. 2019.
[68] P. Hough M. Glaister, and A. Pledger, "The accuracy of wrist-worn heart rate monitors across a range of exercise intensities," *J. Phys. Activity Res.*, vol. 2, no. 2, pp. 112–116, 2017.
[69] C. J. Dondzila *et al.*, "Congruent accuracy of wrist-worn activity trackers during controlled and free-living conditions," *Int. J. Exerc. Sci.*, vol. 11, no. 7, pp. 575–584, 2018.
[70] S. Mehrang, J. Pietilä, and L. Korhonen, "An activity recognition framework deploying the random forest classifier and a single optical heart rate monitoring and triaxial accelerometer wrist-band," *Sensors*, vol. 18, no. 2, p. 613, 2018.

[71] D. J. Plews, P. B. Laursen, J. Stanley, A. E. Kilding, and M. Buchheit, "Training adaptation and heart rate variability in elite endurance athletes: Opening the door to effective monitoring," *Sports Med.*, vol. 43, no. 9, pp. 773–781, Sep. 2013.

[72] I. Mendia-Iztueta, K. Monahan, H. Kyröläine, and E. Hynynen, "Assessment of heart rate variability thresholds from incremental treadmill tests in five cross-country skiing techniques," *PloS One*, vol. 11, no. 1, 2016, Art. no. e0145875.

[73] G. E. Prinsloo, H. G. L. Laurie, and W. D. Derman, "A brief review and clinical application of heart rate variability biofeedback in sports, exercise, and rehabilitation medicine," *Physician Sportsmed.*, vol. 42, no. 2, pp. 88–99, 2014.

[74] M. Malik *et al.*, "Heart rate variability: Standards of measurement, physiological interpretation, and clinical use," *Eur. Heart J.*, vol. 17, no. 3, pp. 354–381, 1996.

[75] E. Gil, M. Orini, R. Bailón, J. M. Vergara, L. Mainardi, and P. Laguna, "Photoplethysmography pulse rate variability as a surrogate measurement of heart rate variability during non-stationary conditions," *Physiol. Meas.*, vol. 31, no. 9, p. 1271, 2010.

[76] A. Bonissi, R. D. Labati, L. Perico, R. Sassi, F. Scotti, and L. Sparagino, "A preliminary study on continuous authentication methods for photoplethysmographic biometrics," in *Proc. IEEE Workshop Biometric Meas. Syst. Secur. Med. Appl.*, Sep. 2013, pp. 28–33.

[77] A. Lourenço, H. Silva, and A. Fred, "Unveiling the biometric potential of finger-based ECG signals," *Comput. Intell. Neurosci.*, vol. 2011, p. 5, Jan. 2011.

[78] T. Nakamura, V. Goverdovsky, and D. P. Mandic, "In-ear EEG biometrics for feasible and readily collectable real-world person authentication," *IEEE Trans. Inf. Forensics Secur.*, vol. 13, no. 3, pp. 648–661, Mar. 2018.

[79] Y. Y. Gu and Y. T. Zhang, "Photoplethysmographic authentication through fuzzy logic," in *Proc. IEEE EMBS Asian-Pacific Conf. Biomed. Eng.*, Oct. 2003, pp. 136–137.

[80] Y. Gu, Y. Zhang, and Y. T. Zhang, "A novel biometric approach in human verification by photoplethysmographic signals," in *Proc. 4th Int. IEEE EMBS Special Topic Conf. Inf. Technol. Appl. Biomed.*, Apr. 2003, pp. 13–14.

[81] P. Spachos, J. Gao, and D. Hatzinakos, "Feasibility study of photoplethysmographic signals for biometric identification," in *Proc. 17th Int. Conf. Digital Signal Process. (DSP)*, Jul. 2011, pp. 1–5.

[82] A. R. Kavsaoğlu, K. Polat, and M. R. Bozkurt, "A novel feature ranking algorithm for biometric recognition with PPG signals," *Comput. Biol. Med.*, vol. 49, pp. 1–14, Jun. 2014, doi: 10.1016/j.compbiomed.2014.03.005.

[83] V. Jindal, J. Birjandtalab, M. B. Pouyan, and M. Nourani, "An adaptive deep learning approach for PPG-based identification," in *Proc. 38th Annu. Int. Conf. IEEE Eng. Med. Biol. Soc. (EMBC)*, Aug. 2016, pp. 6401–6404.

[84] B. P. Krijthe *et al.*, "Projections on the number of individuals with atrial fibrillation in the European Union, from 2000 to 2060," *Eur. Heart J.*, vol. 34, no. 35, pp. 2746–2751, 2013.

[85] C. T. January, *et al.*, "2014 AHA/ACC/HRS guideline for the management of patients with atrial fibrillation: A report of the american college of cardiology/american heart association task force on practice guidelines and the heart rhythm society," *J. Amer. College Cardiol.*, vol. 64, no. 21, pp. e1–e76, 2014.

[86] A. F. Members *et al.*, "2012 focused update of the ESC guidelines for the management of atrial fibrillation: An update of the 2010 ESC guidelines for the management of atrial fibrillation Developed with the special contribution of the European heart rhythm association," *Eur. Heart J.*, vol. 33, no. 21, pp. 2719–2747, Nov. 2012.

[87] D. D. McManus *et al.*, "A novel application for the detection of an irregular pulse using an iPhone 4S in patients with atrial fibrillation," *Heart Rhythm*, vol. 10, no. 3, pp. 315–319, Mar. 2013.

[88] A. G. Bonomi *et al.*, "Atrial fibrillation detection using photoplethysmography and acceleration data at the wrist," in *Proc. Comput. Cardiol. Conf. (CinC)*, Sep. 2016, pp. 277–280.

[89] M. Lemay *et al.*, "Wrist-located optical device for atrial fibrillation screening: A clinical study on twenty patients," in *Proc. IEEE Comput. Cardiol. Conf. (CinC)*, Vancouver, BC, Canada, Sep. 11–14, 2016, pp. 681–684. doi: 10.23919/CIC.2016.7868834.

[90] S. P. Shashikumar, A. M. Shah, Q. Li, G. D. Clifford, and S. Nemati, "A deep learning approach to monitoring and detecting atrial fibrillation using wearable technology," in *Proc. IEEE EMBS Int. Conf. Biomed. Health Inform. (BHI)*, Feb. 2017, pp. 141–144.

[91] M. Saeed *et al.*, "Multiparameter Intelligent Monitoring in Intensive Care II (MIMIC-II): A public-access intensive care unit database," *Critical Care Med.*, vol. 39, no. 5, p. 952, 2011.

[92] *Gyro_Acc_PPG*. Accessed: Mar. 4, 2019. [Online]. Available: https://github.com/hooseok/gyro_acc_ppg

[93] N. Pradhan *et al.*, "Classification of the quality of wristband-based photoplethysmography signals," in *Proc. IEEE Int. Symp. Med. Meas. Appl. (MeMeA)*, May 2017, pp. 269–274.

[94] C.-S. Chu *et al.*, "A finger-free wrist-worn pulse oximeter for the monitoring of chronic obstructive pulmonary disease," *Adv. Biomed. Clin. Diagnostic Surgical Guid. Syst. XIV*, vol. 9698, Jul. 2016, Art. no. 96981C.

Dwaipayan Biswas received the M.Sc. degree in system on chip and the Ph.D. degree in electrical engineering from the University of Southampton (UoS), U.K., in 2011 and 2015, respectively.

He was a Post-Doctoral Research Fellow at UoS, from 2015 to 2016. In 2016, he joined IMEC, as a Researcher on digital IC design for biomedical applications. He has authored 11 journals, over 20 conference publications, and three book chapters. His research interests include low-power VLSI design, biomedical signal processing, machine learning, brain computer interface, and computer architecture.

Neide Simões-Capela received the M.Sc. degree in biomedical engineering from the University of Coimbra, Portugal, in 2013. She is currently pursuing the Ph.D. degree with the University of Leuven, Belgium (KU Leuven), conducting research on modeling psychophysiology toward mental health management, in collaboration with IMEC.

She was with the Group of Electronics and Instrumentation (GEI-Coimbra) on biomedical instrumentation, and later with the Institute for Systems and Robotics (ISR-Coimbra) on stereoscopic imaging.

Chris Van Hoof received the Ph.D. degree in electrical engineering from the University of Leuven, Belgium (KU Leuven), in 1992.

He is the Director of Wearable Healthcare at IMEC and is also a Fellow of IMEC. He has a track record of over 25 years of initiating, executing, and leading national and international contract R&D at IMEC. His work resulted in three startups (two in the healthcare domain) and he has delivered sensor flight hardware to two cornerstone European Space Agency missions. After receiving the Ph.D. from KU Leuven in 1992 in collaboration with IMEC, he has held positions at IMEC as a manager and a director in diverse technical fields (sensors and imagers, MEMS and autonomous microsystems, wireless sensors, body-area networks, and wearable health). He is also a Full Professor at the KU Leuven. He has published over 600 papers in journals and conference proceedings and given over 60 invited talks.

Nick Van Helleputte (M'12) received the M.S. degree in electrical engineering from the University of Leuven, Belgium (KU Leuven), in 2004, and the Ph.D. degree from the MICAS Research Group, KU Leuven, Belgium, in 2009. His Ph.D. research focused on low-power ultra-wide-band analog front-end receivers for ranging applications.

He joined IMEC as an Analog Reseach and Development Design Engineer in 2009, where he is currently a Team Leader of the Biomedical Circuits and Systems Group. His research focuses on ultra-low-power circuits for biomedical applications. He has been involved in analog and mixed-signal ASIC design for wearable and implantable healthcare applications.

Dr. Helleputte served on the technical program committee of VLSI circuits symposium and ISSCC.